

DUAL-BAND CIRCULARLY POLARIZED ANTENNA WITH LOW WIDE-ANGLE AXIAL-RATIO FOR TRI-BAND GPS APPLICATIONS

Y.-Q. Zhang^{*}, X. Li, L. Yang, and S.-X. Gong

National Key Laboratory of Antenna and Microwave Technology, Xidian University, Xi'an, Shaanxi 710071, People's Republic of China

Abstract—This paper presents the design of a dual-band microstrip antenna with low wide-angle axial-ratio. The antenna is designed for global positioning satellite operations at 1227 MHz (L_2), 1575 MHz (L_1) and 1176 MHz (L_5 , available after 2007). This antenna has another advantage of a much wider band in both VSWR and 3 dB axial-ratio compared with single-fed GPS antennas. Details of the design, simulated and experimental results of this GPS antenna are presented and discussed. The measured results confirm the validity of this design, which meet the requirement of GPS applications.

1. INTRODUCTION

Circular polarization (CP) is commonly adopted in GPS and other satellite communications because of the Faraday rotation when signals travel through the ionosphere. Nowadays, the majority of global positioning system (GPS) receivers only operate at L_1 frequency (1575.42 ± 10.23 MHz) with right hand circular polarization, as the L_1 frequency is for civil use. But requiring more precision and reliability, some GPS antennas are requested to cover both L_1 and L_2 (1227.60 ± 10.23 MHz) bands. Modern Global Positioning System introduces the addition of a new navigation signal located at 1176 MHz (L_5) with 24.00 MHz bandwidth for the use of safety of life in 2007.

The circularly-polarized wave can be realized by exciting two linearly polarized modes. These two modes should be with 90° phase difference, equal amplitude, and orthogonal to each other in polarization. There are many types of antenna that can carry out the

Received 17 July 2012, Accepted 5 September 2012, Scheduled 12 September 2012

* Corresponding author: Yun-Qi Zhang (johnny_5@126.com).

CP wave, such as spiral [1]. But the microstrip antennas would be our first choice as it has the advantages of low-profile, light weight and low-cost.

In this paper, we will design a GPS microstrip antenna that performs tri-band CP radiation. Such antenna can be actualized using single feed [2] or dual feeds [3]. The single-feed CP antenna is simple in structure and easy to fabricate, what's more, it requires no feeding network anymore. However the bandwidth is rather too narrow. The 3 dB axial-ratio bandwidth is usually about 20 MHz. Though the bandwidth is enough to the GPS request, but error of machining is ineluctability and this may causes the band excursion. Therefore in this letter dual feeds are adopted to realize the dual-band CP antenna for tri-band GPS applications.

Multifarious microstrip antennas have been presented for GPS applications [4–7]. The proposed antenna in [4] is a dual-band circularly polarized cavity-backed annular slot antenna for GPS receiver with single-feed. Its 10 dB impedance bandwidths are 45 MHz in L_2 and 20 MHz in L_1 , while the 3 dB AR bandwidths are 11 MHz in L_2 and 9 MHz in L_1 . The bandwidth is quite too narrow. An antenna with two patches stacked without an air gap or foam layer is reported in [5]. But the cost of low-temperature cofired ceramic (LTCC) is much too high for large-lot manufacture. The antenna in [6] enhances the bandwidth by applying the stacked structure. However, the bandwidth at L_2 is not broad enough to cover new L_5 band. And a single coaxial probe feed dual-band CP antenna is reported in [7]. But the measured 3 dB axial ratio bandwidth is only 5 MHz.

2. ANTENNA GEOMETRY AND DESIGN

The proposed antenna consists of two stacked patches. And circular patch antenna with two coaxial feeds is considered as a base structure. The feeding network was designed and combined with the antenna.

2.1. Basic Antenna Structure

The geometry of circular patch antenna is shown in Figure 1. Circular polarization can be obtained by two orthogonal modes with 90° phase difference and equal amplitude [8].

For a circular patch, circular polarization for the TM_{110}^Z mode is achieved by using two feeds with proper angular separation, shown in Figure 2. The example is shown in Figure 1 using two coax feeds separated by 90° which generate fields that are orthogonal to each other under the patch, as well as outside the patch. To achieve circular

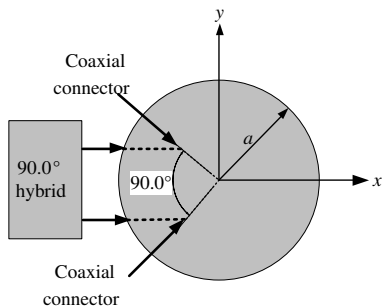


Figure 1. Circular patch arrangement for circular polarization.

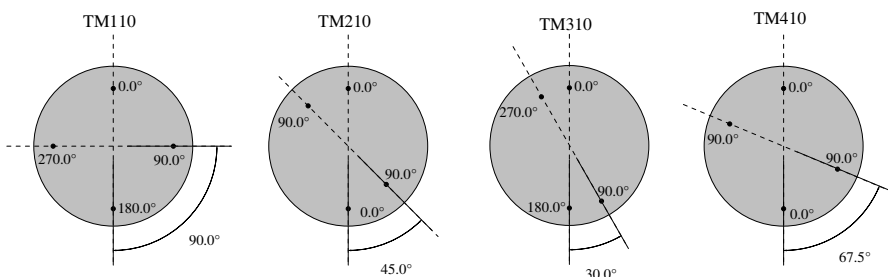


Figure 2. Circular patch feed arrangements for TM_{110}^Z and higher order modes.

polarization, it is also required that the two feeds are fed in such a manner that there is 90° time-phase difference between the fields of the two; this is achieved through the use of a 90° hybrid.

For higher order modes, the spacing between the two feeds to achieve circular polarization is different, as illustrated in Figure 2. The CP antenna with a 90° hybrid is familiar to us all. Various types of 90° hybrid have been reported for circular polarization [9–11].

2.2. Proposed Antenna Design

Figure 3(a) shows the configuration of the proposed antenna. Two circular patches are stacked together on the ground plane. On the bottom of the ground plane, the feeding network is loaded. The antenna is fed by two probes on which the two signals are amplitude equal and phase difference of 90° . On each patch, a cross slot is loaded with different length.

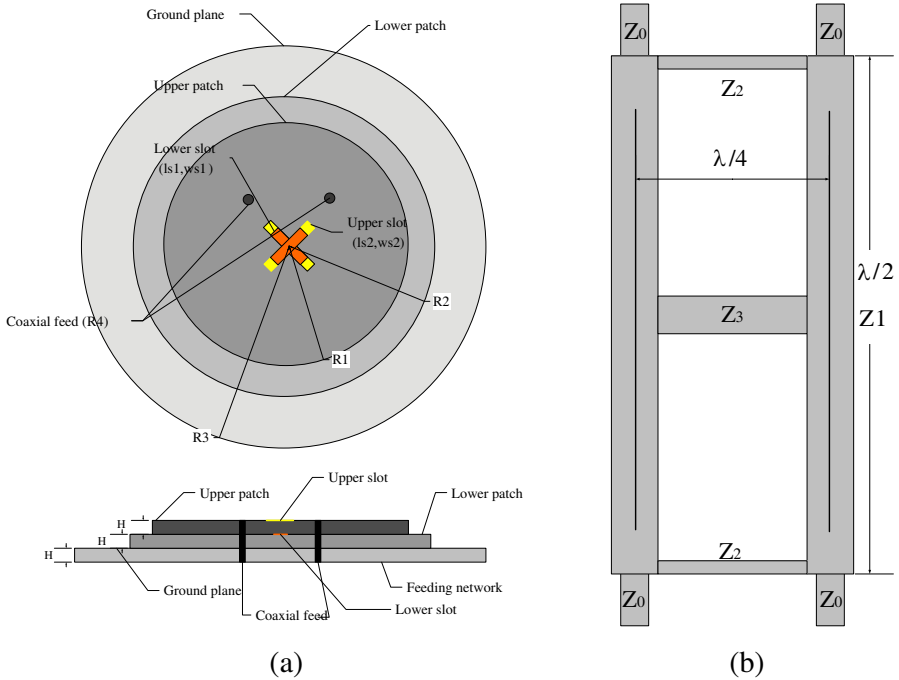


Figure 3. (a) Top and side view of the proposed antenna structure. (b) Branch line directional coupler.

The antenna is fed by two probes, with the same amplitude and different in phase by 90° . And the feeding network is shown in Figure 3(b). The branch line directional coupler is used as it has a wider bandwidth than that of the Wilkinson power divider and 90° phase shifter [12], which will be discussed in Section 3. The geometry of branch line directional coupler is shown in Figure 3(b): $Z_0 = 50 \Omega$, $Z_1 = 38.4 \Omega$, $Z_2 = 126.8 \Omega$, $Z_3 = 47 \Omega$.

This antenna consists three layers with the same height of $H = 2$ mm. All of these three layers use the same substrate of FR4-epoxy ($\epsilon_r = 4.4$, $\tan \delta = 0.02$). For the application of inexpensive substrates, the antenna costs lowly. The radius of ground plane is $R_3 = 64$ mm, while the lower dielectric substrate with a radius of $R_2 = 35$ mm and the upper dielectric substrate of $R_1 = 27$ mm. The length of the slot on the lower patch is $ls_1 = 5$ mm, while that of the upper one is $ls_2 = 9$ mm. The width of these two slots is $ws_1 = ws_2 = 1$ mm. Feed points are $R_4 = 7.2$ mm from the center and they are separated by 90° .

3. SIMULATION AND MEASUREMENT RESULTS

This antenna is designed to cover the three bands of GPS (L_1 , L_2 and L_5), with $50\ \Omega$ input impedance. The gain is supposed to be greater than 0 dBi. As the L_2 and L_5 frequencies are closed to each other, we are possible to achieve the goals using a dual band antenna with L_2 and L_5 within the same band. The antenna without the feeding network and slots is simulated first. The antenna is designed and optimized by HFSS.

Figure 4 shows the S_{11} of the antenna with different height of the substrate. Seen from the figure that the thicker the substrate is, the wider the band will be. We choose the height of 2 mm as it's more common in use. Figure 5 shows the S_{11} with the variety of R_1 when $R_2 = 35$ mm. It is noted that when $R_1 = 27$ mm, the higher resonance frequency meets L_1 band. Figure 6 shows that when $R_1 = 27$ mm, the lower resonance frequency varies with R_2 . The lower resonance frequency is nearly equal to L_2 band as $R_2 = 35$ mm. Figure 7 shows the axial-ratio of the antenna without feeding network and slots. Within the whole band, the axial-ratio is below 3 dB as it's fed perfectly.

As mentioned in Section 2.2, the Wilkinson power divider and 90° phase shifter may also be used as the feeding network, shown in Figure 8. The simulation results of different feeding networks are shown in Figure 9. The antenna is optimized due to different feeding networks. As shown in Figure 9(a), the S_{11} of the antenna with Wilkinson power divider and 90° phase shifter is about -7 dB at L_1 band. It's obvious that the branch line directional coupler provides a wider VSWR band.

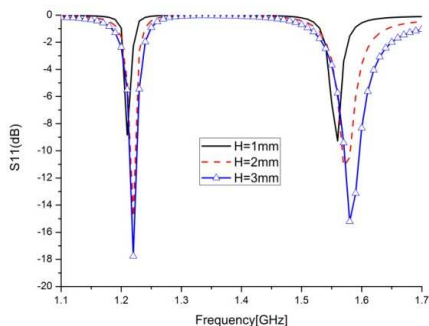


Figure 4. S_{11} of $H = 1$ mm, 2 mm and 3 mm.

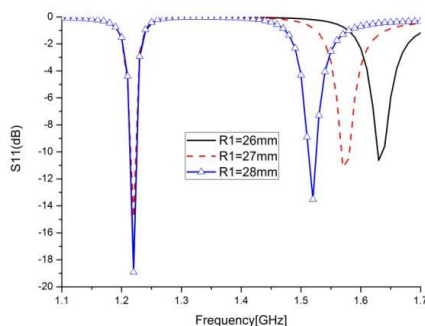


Figure 5. S_{11} of $R_1 = 26$ mm, 27 mm and 28 mm, $R_2 = 35$ mm.

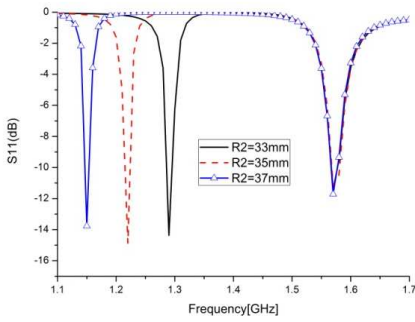


Figure 6. S_{11} of $R_2 = 33$ mm, 35 mm and 37 mm, $R_1 = 27$ mm.

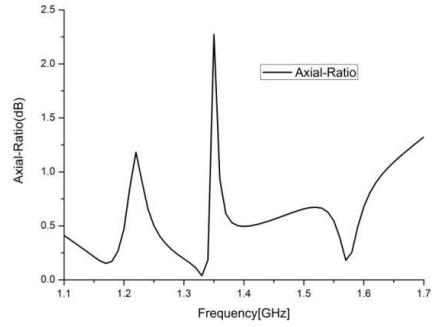


Figure 7. Axial-Ratio of the antenna without feeding network.

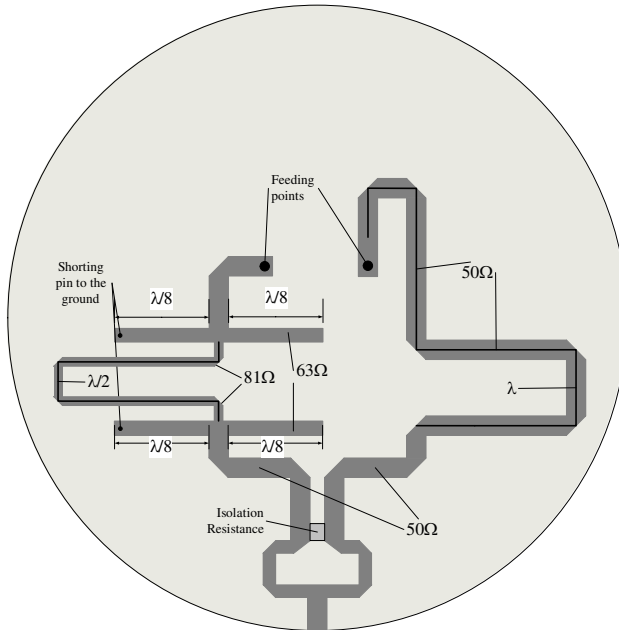


Figure 8. Wilkinson power divider and 90° phase shifter.

The results of AR are shown in Figure 9(b), the AR of Wilkinson power divider doesn't meet the demand of $AR < 3$ dB at L_5 and L_2 band. So in this paper, we choose the branch line directional coupler as the feeding network.

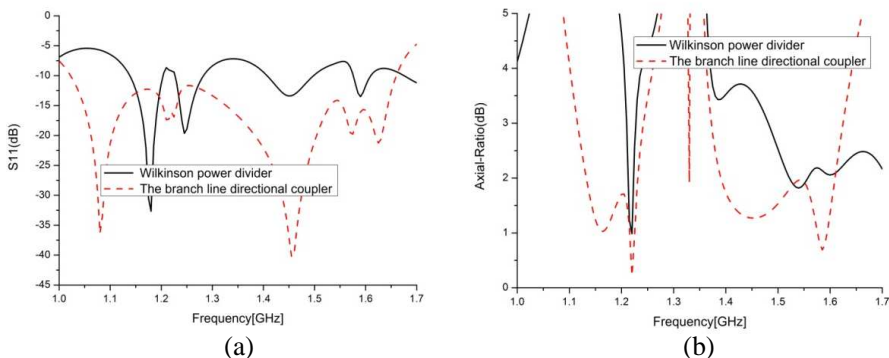


Figure 9. (a) S_{11} of different feeding network. (b) Axial-ratio.

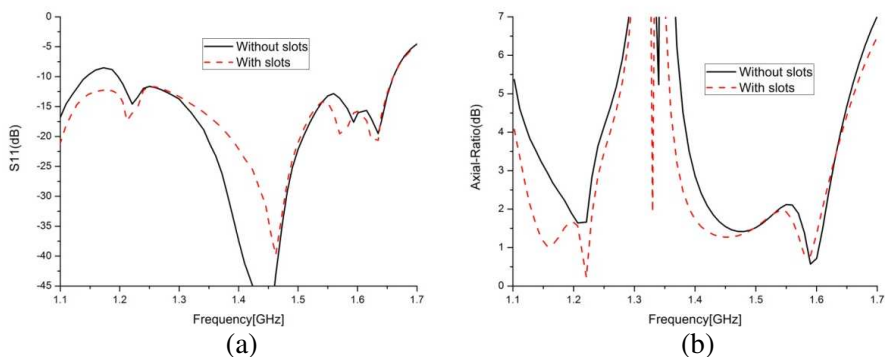


Figure 10. (a) S_{11} . (b) Axial-ratio.

The simulation results of the antenna with and without slots are shown in Figure 10 (with feeding network). As noted the 3 dB axial-ratio bandwidth of the antenna without slots is not below 3 dB at L_5 band. And the S_{11} is about -11 dB at L_1 band and -7 dB at L_5 band. Universally acknowledged, the antenna can be practically used when $S_{11} < -10$ dB.

Figure 11 shows the variation of the S_{11} and axial-ratio with different size of the upper slot. As noted in Figure 11(a), the S_{11} of $l_{s2} = 7$ mm approaches to -10 dB at L_1 band. And shown in Figure 11(b), the axial-ratio of $l_{s2} = 11$ mm is not below 3 dB at L_1 band. So the length of upper slot is optimized to $l_{s2} = 9$ mm.

For the lower slot, the influence of l_{s1} is shown in Figure 12. As noted, the S_{11} of $l_{s1} = 3$ mm is about -9 dB at L_1 band, and that

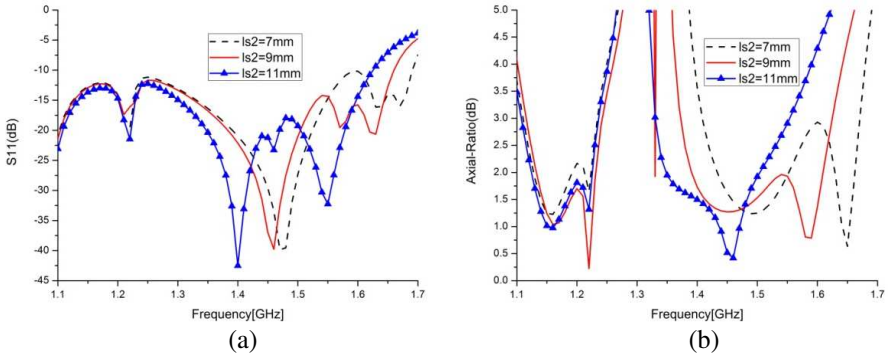


Figure 11. (a) S_{11} . (b) Axial-ratio.

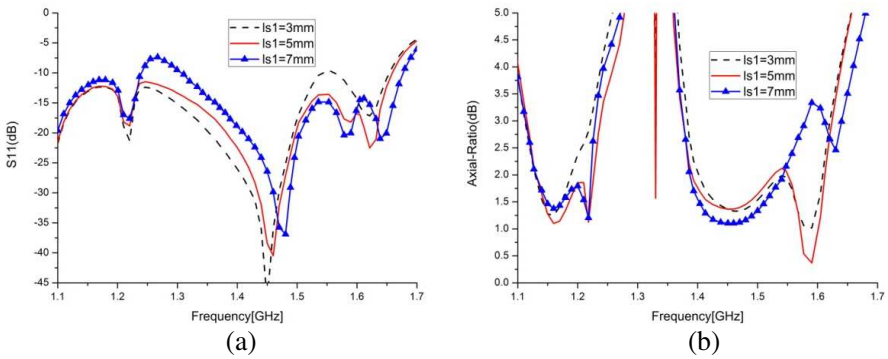


Figure 12. (a) S_{11} . (b) Axial-ratio.

of $l_{s1} = 7$ mm is -7 dB at L_2 band. What's more, the axial-ratio of $l_{s1} = 7$ mm is nearly 3.5 dB at 1580 MHz. So the length of lower slot is optimized to be 5 mm. Both of the width of these two slots are also optimized. And when $w_{s1} = w_{s2} = 1$ mm, it provides the best simulation results.

The position of the probe feeds are illustrated too. As shown in Figure 13(a), the S_{11} of $R_4 = 6$ mm is close to -10 dB at L_1 band. While that of $R_4 = 8$ mm and $R_4 = 9$ mm is about -8 dB at L_2 band. Figure 13(b) shows the variation of axial-ratio with R_4 . It's obvious that when $R_4 = 8$ mm and $R_4 = 9$ mm, the axial-ratio are higher than 3 dB at 1230 MHz. Finally, R_4 is determined to be 7.2 mm.

The actual prototype is shown in Figure 14. The simulated and measured VSWR of the designed dual-fed dual-band CP antenna are

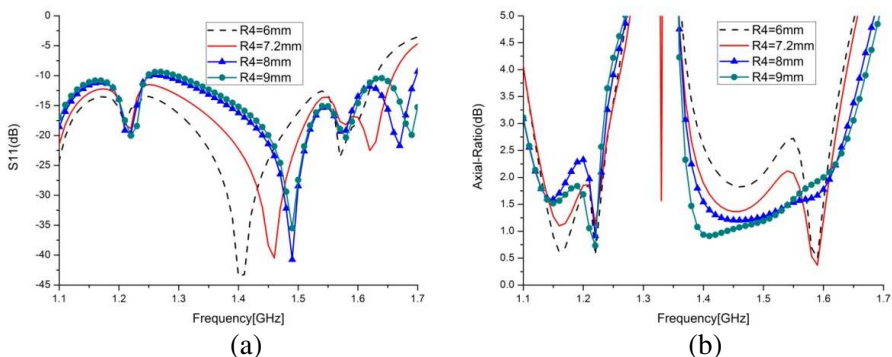


Figure 13. (a) S_{11} . (b) Axial-ratio.



Figure 14. Top view, back view and side view of the proposed antenna.

shown in Figure 15. As shown, the measured and simulated data are in good agreement. The measured bandwidth of $VSWR < 2$ is 49.7% (1019 MHz to 1693 MHz). Comparing to the simulated result of impedance band, the measured shift right a little at L_1 band. For the CP microstrip antenna, the most attractive characteristic is AR . The simulated and measured axial-ratio are shown in Figure 16. The measured results match well with the simulated results. The measured bandwidth of $AR < 3\text{ dB}$ is 13.8% at L_5 and L_2 band (1079 MHz to 1239 MHz), and 14.9% at L_1 band (1389 MHz to 1614 MHz).

Figure 17 show the wide angle axial-ratio at 1180 MHz (L_5), 1230 MHz (L_2) and 1580 MHz (L_1). The simulated and measured wide angle AR are chosen on the XoZ plane ($\phi = 0^\circ$). As shown,

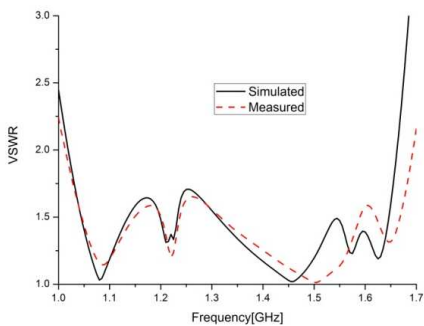


Figure 15. Simulated and measured VSWR.

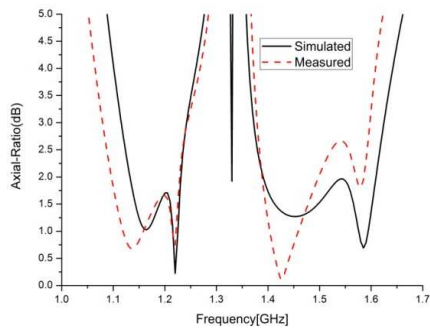
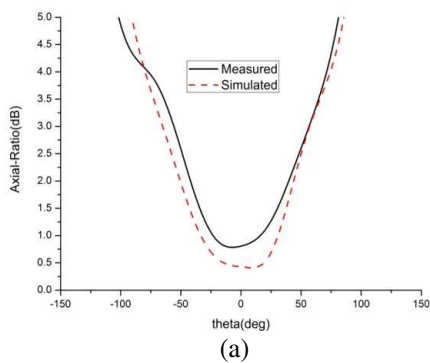
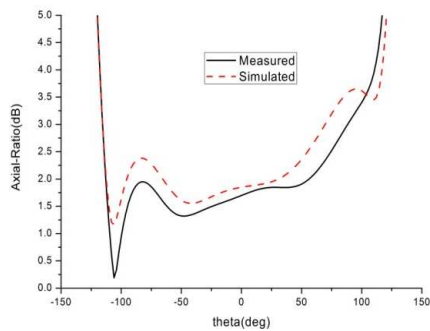


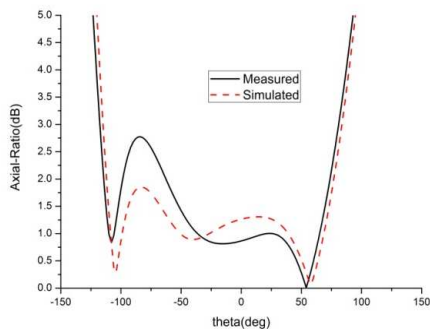
Figure 16. Simulated and measured AR.



(a)



(b)



(c)

Figure 17. Wide angle AR of each band (a) L_1 , (b) L_2 , (c) L_5 .

the bandwidth of wide angle $AR < 3$ dB is about 200° at both L_2 and L_5 band, and at the L_1 band it is about 120° . It's much wider than the single-feed CP antenna, and it will be of great help in reducing the influence of multipath effect.

The measured RHCP radiation patterns in two orthogonal planes (XoZ and YoZ) are plotted in Figure 18. And these radiation patterns were measured at the frequencies of 1180 MHz (L_5), 1230 MHz (L_2) and 1580 MHz (L_1). As expected, the proposed design achieves good broadside CP radiation patterns at each frequencies. The measured gain for these three band are 6.2 dBi (1180 MHz, L_5), 6.9 dBi (1230 MHz, L_2), 7.7 dBi (1580 MHz, L_1). A comparison of the demands of modern GPS antenna with the measured results is shown in Table 1.

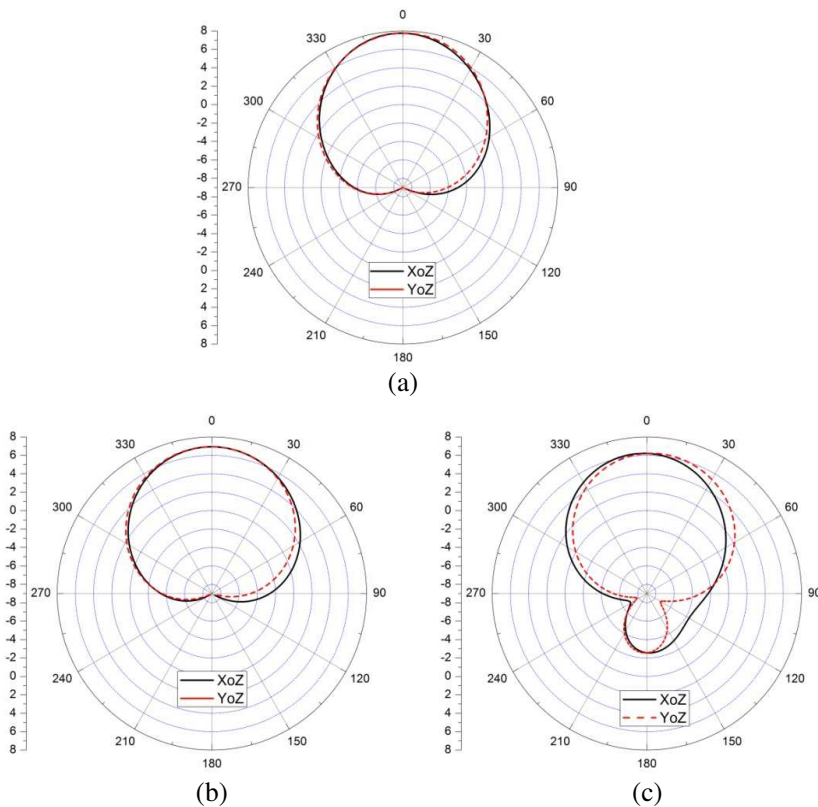


Figure 18. Radiation pattern of each frequency (a) 1580 MHz, (b) 1230 MHz, (c) 1180 MHz.

Table 1. A comparison of demands with measured results.

Parameter	VSWR	Gain	Axial-Ratio
Demands of modern GPS	VSWR < 2	Gain > 0 dBi at each band	AR < 3 dB
	1164–1188 MHz		1164–1188 MHz
	1217–1237 MHz		1217–1237 MHz
	1565–1585 MHz		1565–1585 MHz
Measured results in the paper	VSWR < 2 from 1019 MHz to 1693 MHz	1180 MHz: 6.2 dBi 1230 MHz: 6.9 dBi 1580 MHz: 7.7 dBi	AR < 3 dB 1079–1239 MHz 1389–1614 MHz

4. CONCLUSION

This paper introduces a new design of dual-feed dual-band circularly polarized antenna for tri-band GPS applications (transmitter or receiver). Compared to the conventional single-feed CP antenna, this antenna owns wider bandwidth in both VSWR and axial-ratio. In addition, the volume is small and the cost low. We present the function of the applied slots in axial-ratio and S_{11} at L_5 band. From the measured results, it is seen that the proposed antenna achieves good dual-band CP performance, which meets the requirement of GPS applications at the L_1 , L_2 and L_5 bands.

REFERENCES

1. Padros, N., J. Ortigosa, J. Baker, M. Iskander, and B. Thomborg, "Comparative study of high-performance GPS receiving antenna design," *IEEE Trans. Antennas and Propagation*, Vol. 45, No. 4, 698–706, 1997.
2. Heidari, A. A., M. Heyrani, and M. Nakhkash, "A dual-band circularly polarized stub loaded microstrip patch antenna for GPS applications," *Progress In Electromagnetics Research*, Vol. 92, 195–208, 2009.
3. Zhou, Y., C.-C. Chen, and J. L. Volakis, "Dual band proximity-fed stacked patch antenna for tri-band GPS applications," *IEEE Trans. Antennas and Propagation*, Vol. 55, No. 1, 220–223, Jan. 2007.
4. Hsieh, W.-T., T.-H. Chang, and J.-F. Kiang, "Dual-band circularly polarized cavity-backed annular slot antenna for GPS receiver," *IEEE Trans. Antennas and Propagation*, Vol. 60, No. 4, 2076–2080, Apr. 2012.

5. Chen, S., G. Liu, X. Chen, T. Lin, X. Liu, and Z. Duan, "Compact dual-band GPS microstrip antenna using multilayer LTCC substrate," *IEEE Antennas and Wireless Propagation Letters*, Vol. 9, 421–423, 2010.
6. Wang, Y., J. Feng, J. Cui, and X. Yang, "A dual-band circularly polarized stacked microstrip antenna with single-fed for GPS applications," *Antenna, Propagation and EM Theory, ISAPE 2008*, 108–110, 2008.
7. Beddeleem, G., J. M. Ribero, G. Kossiavas, R. Staraj, and E. Fond, "Dual-frequency antenna circularly polarized for GPS-SDARS operation," *Antennas and Propagation, EuCAP 2007*, 1–5, 2007.
8. Huang, J., "Circularly polarized conical patterns from circular microstrip antennas," *IEEE Trans. Antennas and Propagation*, Vol. 32, No. 9, 991–994, Sep. 1984.
9. Chiu, L. and Q. Xue, "Investigation of a wideband 90° hybrid coupler with an arbitrary coupling level," *IEEE Trans. Microwave Theory and Techniques*, Vol. 58, No. 4, 1022–1029, Apr. 2010.
10. Gipprich, J. W., "A new class of branch-line directional couplers," *IEEE MTT-S International Microwave Symposium Digest*, Vol. 2, 589–592, 1993.
11. Tanaka, H., N. Babba, S. Arai, and T. Nishikawa, "2 GHz one octave-band 90 degree hybrid coupler using coupled meander line optimized by 3-D FEM," *IEEE MTT-S International Microwave Symposium Digest*, Vol. 2, 903–906, 1994.
12. Eom, S. Y. and H. K. Park, "New switch=network phase shifter with broadband characteristics," *Microwave Optical Technology Letter*, 255–257, 2003.